Uptake of Gas-Phase Nitrous Acid by pH-Controlled Aqueous Solution Studied by a Wetted Wall Flow Tube

Jun Hirokawa,* Takehiro Kato,† and Fumitaka Mafuné†

Faculty of Environmental Earth Science, Hokkaido University, Kita-10, Nishi-5, Sapporo, 060-0810, Japan

Received: June 11, 2008; Revised Manuscript Received: August 21, 2008

Uptake kinetics of gas phase nitrous acid (HONO) by a pH-controlled aqueous solution was investigated by using a wetted wall flow tube. The gas phase concentration of HONO after exposure to the aqueous solution was measured selectively by the chemical ionization mass spectrometer in a high sensitive manner. The uptake rate of the gaseous HONO was found to depend on the pH of the solution. For the uptake by neutral and alkaline solutions, the gas phase concentration was observed to decay exponentially, suggesting that the uptake was fully limited by the gas phase diffusion. On the other hand, the uptake by the acidic solution was found to be determined by both the gas phase diffusion and the liquid phase processes such as physical absorption and reversible acid dissociation reaction. The decay was analyzed by the rate equations using the time dependent uptake coefficient involving the saturation of the liquid surface. While the uptake processes by the solution at pH = 2−3 were well described by those calculated using the physical and chemical parameters reported for the bulk, the uptake rates by the solution at $4 < pH < 7$ deviate from the calculated ones. The present result can suggest that the pH at the liquid surface is lower than that in the bulk liquid, which is responsible for the additional resistance of mass transfer from the gas to the liquid phase.

1. Introduction

Heterogeneous processes between atmospheric trace species and liquid aerosols play a significant role in both the tropospheric and stratospheric chemistry. These processes are characterized by the mass transfer across the interface from the gas to the liquid phase. The rate of the interfacial mass transfer can be described in terms of the mass accommodation coefficient α, which is defined as a fraction of collisions of a gas-phase molecule with a liquid surface that results in incorporation of the molecule into the liquid. The uptake processes actually observed in the atmosphere can, however, involve not only the interfacial mass transfer but also other elementary steps including the diffusion in the gas phase and the physical absorption and the chemical reactions in the liquid phase. In addition to these gas and liquid phase processes, recent experimental and theoretical studies suggest that there are chemical reactions characteristic to the interface which cause the uptake rate to change more or less.[1−3]

Nitrous acid is an important trace species in tropospheric chemistry because it is known to be photolyzed by sunlight to produce a hydroxyl radical (OH), a major oxidizing agent in the troposphere. In both the production and removal of the tropospheric HONO, the heterogeneous processes have been suggested to play a significant role. For the production of HONO, various heterogeneous reactions involving NO_2 has been proposed.[4−6] Among them, the reaction of NO_2 with water on wet surfaces is believed to be important

$$2NO_2 + H_2O \rightleftarrows HONO + HNO_3 \quad (1)$$

On the other hand, observational studies suggest that the uptake of HONO by aqueous particles such as cloud droplets may act as its important removal process.[7] For the uptake of HONO by liquid water, several studies have been performed with the aim of determining the accommodation coefficient, α, which is reported to be in the range between 10^{-3} and 10^{-1} at temperatures ranging from 245 to 297 K.[8,9] However, the uptake of HONO by the aqueous solution proceeds via the accommodation process followed by the physical absorption

$$HONO\ (g) \rightleftarrows HONO\ (aq) \quad (2)$$

and the reversible acid dissociation reaction

$$HONO\ (aq) \rightleftarrows NO_2^-\ (aq) + H^+\ (aq) \quad (3)$$

where (g) and (aq) denote the species in the gas and aqueous phases, respectively. These processes can have an effect on the net transfer rate of HONO from the gas to the liquid phase. Therefore, the net transfer rate is described in terms of the uptake coefficient, which is generally different from the accommodation coefficient. Especially, the uptake coefficient that is determined by these reversible processes decreases with an increase in the gas−liquid contact time, approaching 0 at the infinite contact time, when the solution is fully saturated, that is, the equilibrium has been established. In fact, it is indicated that the measurements of the accommodation coefficient are subjected to significant surface saturation,[3,10] resulting in reported values much lower than the true α. Recent theoretical studies suggest that the accommodation coefficients for hydrophilic species are close to unity.[11]

Here we focus our attention on the liquid phase processes rather than the mass accommodation process to determine the uptake rate of HONO. In order to elucidate them, we examined the uptake of HONO by a pH-controlled aqueous solution because reversible acid dissociation can be controlled by the pH. As the uptake rate controlled by eqs 2 and 3 is expected to depend on the contact time due to the surface saturation, we measured the time-dependent uptake by the flow tube technique

* To whom correspondence should be addressed. E-mail: hirokawa@ees.hokudai.ac.jp.

† Permanent address: Department of Basic Science, School of Arts and Sciences, The University of Tokyo, Komaba, Meguro, Tokyo 153-8902, Japan.

10.1021/jp8051483 CCC: $40.75 © 2008 American Chemical Society
Published on Web 11/04/2008

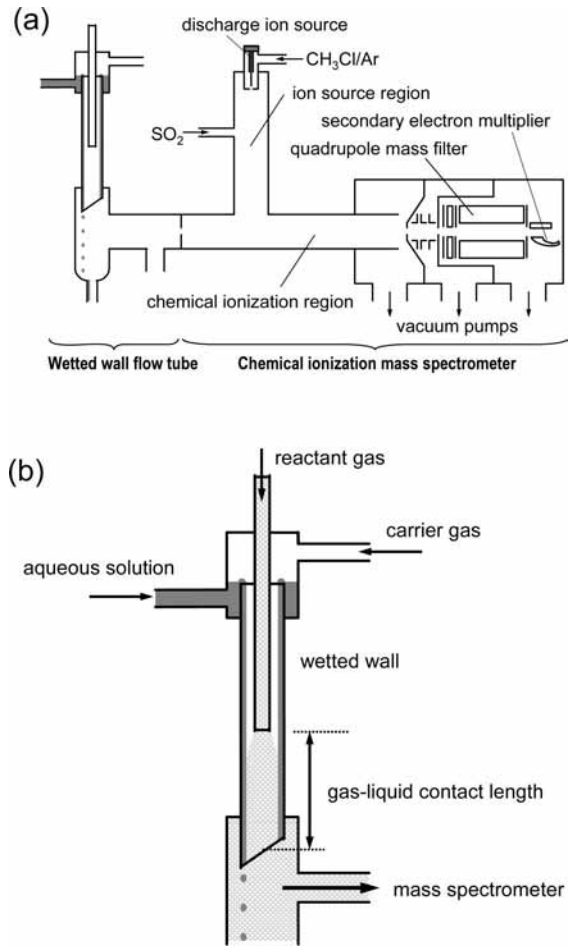

Figure 1. (a) Schematic diagram of experimental apparatus used in the present study. (b) Wetted wall flow reactor.

and compared the experimental data with those calculated from the rate equation for the HONO uptake explicitly including the contact-time dependence of the uptake coefficient.

2. Experimental Section

2.1. Wetted Wall Flow Tube. A schematic diagram of the apparatus used in the present study is shown in Figure 1a. The apparatus consists of a wetted wall flow tube coupled to the chemical ionization mass spectrometer. The wetted wall flow tube used in this study, which is shown in Figure 1b, is similar to those used in the previous studies by other groups.[12,13] It consists of a vertically aligned Pyrex glass tube with an internal diameter of 2.0 cm and a length of 80 cm. On the inner surface of the tube, a liquid film was formed by an aqueous solution for the uptake of HONO. The aqueous solution was supplied to the reservoir located at the top of the flow tube from a closed glass vessel, in which the solution was pressurized at ~1.1 atm by N_2, by their pressure difference. When the reservoir was filled, the solution spilled over the reservoir edge and flowed downward along the vertical wall under the effect of gravity. The internal surface of the glass flow tube was kept so hydrophilic that the entire surface was wetted uniformly by the flowing thin liquid film. For this purpose, the inside wall of the flow tube was occasionally cleaned with a detergent solution, followed by thorough rinsing with deionized water. It was also important that the flow tube was filled with deionized water while not in use. The liquid flow rate was regulated by a needle valve before entering the reservoir at 20 mL min^{-1}, which gives the liquid flow velocity at the gas−liquid interface, v, as 6.8 cm s^{-1}.[14] The Reynold's number of the liquid flow was about 30, which is slightly higher than the Reynold's number of the laminar flow ($\leq$10). Actually small rippling was observed. This could lead to overestimation of the binary diffusion coefficients reported in this study as mentioned in section 3.2. The solution after the flow tube was removed readily to a storage tank located downward of the flow tube through a 20-cm-long Teflon tube.

A flow of the He carrier gas was introduced into the flow tube after humidified by passing through a water bubbler in order to avoid the evaporation of water from the liquid film. The flow rate of the carrier gas was controlled at 3600 STP (standard temperature and pressure) cm^3 min^{-1} by a calibrated thermal mass flow controller. Another flow of the He gas containing trace amounts of HONO prepared as described in section 2.3 was introduced through a movable injector with an internal diameter of 0.6 cm, which is inserted to the flow tube in a coaxial configuration. HONO thus introduced was allowed to interact with the flowing liquid surface. We changed the gas−liquid contact length or the contact time by sliding the gas injector position vertically with respect to the flow tube. The total gas flow rate yields the average flow velocity, $\bar{u}$, as 21.4 cm s^{-1} and the Reynold's number of the gas flow as about 30. A part of the gas flow after the flow tube was extracted through a 0.25-mm-diameter pinhole into the chemical ionization mass spectrometer for analysis. The other part was removed by a diaphragm pump through a port located between the flow tube and the chemical ionization mass spectrometer. A needle valve located before the diaphragm pump controlled the total pressure inside the flow tube at 760 Torr. Although the temperature of the flow tube was not actively regulated, the temperature measured before and after runs ranged between 294 ± 1 K. Hence, we adopted the temperature of 294 K for the data analysis.

2.2. Chemical Ionization Mass Spectrometer. The chemical ionization mass spectrometer consists of three regions: ion source region, chemical ionization region, and mass analysis region. At the top of the ion source, Cl^- was generated by the discharge of the CH_3Cl/Ar gas mixture. Then Cl^- attached to SO_2, which was introduced via a side port of the ion source region to produce the reagent ion for the chemical ionization, SO_2Cl^-, in the presence of Ar as the third body. The flow of the reagent ion entered the chemical ionization region and was mixed with the gas flow extracted from the flow tube. HONO was ionized via the following reversible reaction:

$$HONO + SO_2Cl^- \rightleftarrows HONOCl^- + SO_2 \qquad (4)$$

After the chemical ionization, ions including the product ions and unreacted SO_2Cl^- were introduced into the mass analysis region, where the ions were mass-analyzed by the quadrupole mass filter and detected by the secondary electron multiplier. Ion signals at a certain mass-to-charge ratio (m/z) were recorded as the count rate (counts per second, cps). As shown in section 3.1, it was confirmed that the ratio of the count rate for $HONOCl^-$ to that for SO_2Cl^- was proportional to the HONO concentration in the gas phase. Hence, the count rates recorded by the mass spectrometer give the HONO concentration in the flow tube.

2.3. Preparations of HONO and Aqueous Solutions. Nitrous acid was synthesized by adding $NaNO_2$ powder into acidic solution buffered at pH = 4 in the closed flask via the one pot chemical reaction

$$NaNO_2 + H^+ \rightarrow Na^+ + HONO \qquad (5)$$

Because the amounts of HONO produced in the gas phase change sensitively with the temperature of the solution, the

temperature of the flask was kept at 288 K using a cooling bath. The prepared HONO was entrained in the He gas flow controlled by a mass flow controller located upstream of the flask. Typical flow rate of the He gas was 400 STP cm^3 min^{-1}. The resultant HONO/He gas mixture was carried into the flow reactor through the movable injector as described in section 2.1. It should be noted that the reactant gas flow was humidified by the water in the one-pot reactor.

Although the method to prepare HONO by the reaction between $NaNO_2$ and acids has been used by other studies,[15−17] it is also indicated that byproducts such as NO and NO_2 can be formed upon preparation.[15,16] The presence of NO_2 in the reactant gas would interfere with the uptake measurement by eq 1. In addition, NO can have an effect on the uptake of HONO if it coexists with NO_2 because the following reaction can occur to produce HONO:

$$NO + NO_2 + H_2O \rightleftarrows 2HONO \quad (6)$$

Hence, it is important to quantify the NO and NO_2 concentrations in the reactant gas flow. We measured the concentrations of NO and NO_2 in the gas in the flow tube by a chemiluminescence NO_x analyzer. Here, NO was directly monitored, while NO_2 after being converted to NO with a catalytic converter. In practice, HONO is also converted to NO and detected by the NO_x analyzer efficiently (>95%).[18] Therefore, the total concentration of NO, NO_2, and HONO was obtained by the chemiluminescence detector after the converter. Then, NO_2 and HONO were distinguished by removing HONO selectively by the liquid water, because the Henry's law solubility of HONO is 3 orders of magnitude higher than that of NO_2. By examining the gas mixture in these three modes, the concentrations of NO, NO_2, and HONO were obtained individually. Typical concentrations of HONO and NO were measured to be 1.1×10^{12} and 3.5×10^{11} molecules cm^{-3}, respectively, whereas that of NO_2 was found to be under the detection limit. Kleffmann et al.[19] reported that the forward reaction of eq 6 is negligible for the NO concentration up to 5×10^{13} molecules cm^{-3}. Therefore, the consumption of NO_2 and the production of HONO by eq 6 can be neglected at this NO level. The fact that the NO_2 was not detected by the NO_x analyzer shows that NO_2 was not produced upon preparation of HONO in this study, and hence, we can ignore the interference of NO_2 in the uptake measurements via eq 1. The effect of NO is also insignificant because NO is inactive with water in the absence of NO_2. Hence, the HONO concentration was not monitored by the NO_x analyzer during the uptake measurements. The backward reaction of eq 6 is also considered to be insignificant because of low concentration of HONO prepared in this study. Indeed, no appreciable difference in the uptake was observed when we varied the initial concentration of HONO between 10^{11} and 10^{13} molecules cm^{-3}. This finding suggests that the self-reaction of HONO such as the backward reaction of eq 6 is negligible. In addition, it is indicated that only the relative change of the HONO concentration is used in the analysis of the uptake rate as outlined in the next section.

The solution for the uptake of HONO was prepared from deionized water. The solutions at pH = 2.1 and 3.0 were prepared by diluting sulfuric acid (H_2SO_4) with water. The solution at pH = 4.4 was prepared using potassium hydrogen phthalate ($KHC_8O_4H_4$) buffer, whereas solutions at pH = 5.3 and 7.1 were prepared using potassium dihydrogenphosphate (KH_2PO_4)/disodium hydrogenphosphate (Na_2HPO_4) buffer. The solution at pH = 11.1 was prepared by dissolving sodium hydroxide (NaOH) in water. The pH of the prepared solution was measured by a pH meter before and after every uptake measurement. To remove dissolved O_2, the solution was bubbled by N_2 prior to each experiment.

2.4. Data Analysis for a Wetted Wall Flow Tube. In the wetted wall flow tube as well as in the atmosphere, the uptake rate is determined by several elementary steps such as the interfacial mass transfer, the gas phase diffusion, and the physical and chemical processes in the bulk liquid. In this section, we derive the rate equation for the uptake of HONO and describe the procedure to analyze the experimental data obtained by the wetted wall flow tube.

The removal of HONO by the liquid film on the wall is characterized by the uptake coefficient, γ_w, which is defined as a fraction of collisions to the wall surface that results in the removal of the species from the gas phase. When the gas phase diffusion is so fast that the HONO concentration is uniform along the radial direction (which corresponds to the plug flow condition), the decay rate of HONO in the gas phase is determined only by the wall loss processes. In this case, the rate equation in the laminar flow condition is described as[20]

$$\frac{d[HONO]}{dt} = -\frac{\gamma_w \omega}{2r}[HONO] \quad (7)$$

where r is the radius of the flow tube and ω is the average thermal speed of the HONO molecules in the gas phase. If we assume that the accommodation coefficient, α, is unity, γ_w is determined only by the physical absorption (eq 2) and the acid dissociation reaction (eq 3). When the equilibriums are established for eq 2 at the gas−liquid interface and for eq 3 at any points in the liquid phase in the course of the uptake, γ_w is given as[14,21,22]

$$\gamma_w = \frac{4H_{eff}RT}{\omega}\sqrt{\frac{D_{aq}\upsilon}{\pi z}} = \frac{4H_{eff}RT}{\omega}\sqrt{\frac{D_{aq}}{\pi t'}} \quad (8)$$

where R is the gas constant, T is the temperature, υ is the velocity of the flowing liquid at the gas−liquid interface, z is the gas−liquid contact length, and $t' = z/\upsilon$ is the contact time for the liquid with the gas. The effective Henry's law coefficient, H_{eff}, is defined by

$$H_{eff} = H\left(1 + \frac{K_a}{[H^+]}\right) \quad (9)$$

where H and K_a are the Henry's law coefficient and acid dissociation constant of HONO, respectively, and $[H^+]$ is the proton concentration in the liquid. Equation 8 shows that γ_w decreases with the contact time, t', and approaches zero at $t' = \infty$, when the solution becomes fully saturated with HONO(aq).

In the other extreme case where the gas phase diffusion totally limits the mass transfer rate, the HONO concentration, which varies with the radial direction as well as the axial direction, is given by the continuity equation with the boundary condition that the HONO concentration is equal to zero at the wall surface. The analytical solution of this equation, which is referred to as the Gomeley−Kennedy (GK) solution by Murphy and Fahey,[23] can be approximated by the single exponential form at relatively long contact time. If [HONO] is redefined as the HONO concentration averaged over the cross section of the tubular flow reactor, this is described as

$$[HONO] = 0.819[HONO]_0 \exp\left(-\frac{3.657D_g}{r^2}t\right) \quad (10)$$

where D_g is the gas phase diffusion coefficient for HONO in the carrier gas mixtures and $[HONO]_0$ is the initial concentration of [HONO] before exposure to the liquid wall.

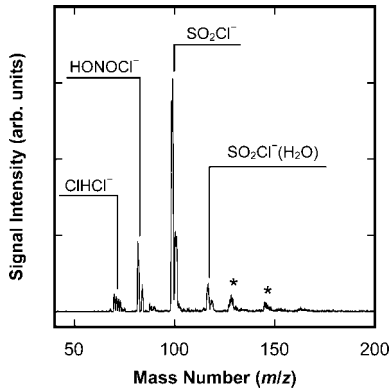

Figure 2. Typical mass spectrum of ions observed by the chemical ionization mass spectrometer. Peaks at $m/z = 128$ and 146 (marked by *) were hardly assignable to the specific ions.

In the present experiments operated under atmospheric pressure, however, we need to consider intermediate cases between two extremes. Also in these cases, the HONO concentration changes with the radial direction, and hence, is governed by the continuity equation, though the boundary condition is different from that for the diffusion limited case: The boundary condition is related to the wall loss processes. The analytical solution of the equation is referred to as the Cooney−Kim−Davis (CKD) solution by Murphy and Fahey, who presented the solution for a given value of γ_w.[23] On the other hand, Brown[24] presented the algorithm to correct the experimentally observed decay for the effects of the gas phase diffusion by solving numerically the continuity equation with the same boundary condition. Very recently, Davis[25] presented more generalized treatment of the continuity equation for the flow tube experiments and reanalyzed the data that have been obtained previously by several research groups. Although the algorithm of Brown or the solution presented by Murphy and Fahey has been utilized to obtain true γ_w by several groups using wetted wall flow tubes,[12,26−28] it is still difficult to apply these methods to the present study, because γ_w can vary with the contact time. Thus we adopted an alternative approach, which has been applied to the studies using the wetted[13,29,30] or coated wall flow tubes.[31,32] The starting point is the assumption that the decay of the gas phase HONO can be described as the rate equation similar to eq 7, which is known to be valid under the plug flow condition. Using [HONO] as the HONO concentration averaged over the cross section of the flow tube, the rate equation is written as

$$\frac{d[HONO]}{dt} = -\frac{\gamma_{tot}\omega}{2r}[HONO] \quad (11)$$

where γ_{tot} is the overall uptake coefficient, which includes the effects of both the gas phase diffusion and the wall loss processes. Then, γ_{tot} is assumed to be given based on the resistance model as[33,34]

$$\frac{1}{\gamma_{tot}} = \frac{1}{\gamma_d} + \frac{1}{\gamma_w} \quad (12)$$

where $1/\gamma_{tot}$ corresponds to the total resistance for the mass transfer from the gas to the liquid phase, which is given by the summation of the gas-phase diffusive resistance, $1/\gamma_d$, and the resistance of the wall loss processes, $1/\gamma_w$. Considering the case where $\gamma_d \ll \gamma_w$, γ_{tot} is nearly equal to γ_d, which is, in turn, found to be expressed in terms of the diffusion coefficient, D_g, from eqs 10 and 11 as

$$\gamma_d = \frac{2\times 3.657}{\omega r} D_g \quad (13)$$

On the other hand, γ_w is given as eq 8, indicating that γ_w, and hence γ_{tot}, depends on the contact time. Then eq 11 should be integrated with taking the time dependence of γ_{tot} into account. It should be noted that at a certain contact length (z) the contact time for the liquid, t', is different from that for the gas, t, because of the difference in their flow velocities. Since the rate equation 11 is written in terms of the contact time for the gas, the contact time for the liquid in eq 8 should be converted to that for the gas when it is substituted into eq 11. This conversion can be done by using the relation $z = \bar{u}t = vt'$. Substituting eqs 8 and 13 into eq 11 with the conversion of t' to t gives the following form of the rate equation:

$$-\frac{d[HONO]}{dt} = \frac{A}{1+Bt^{1/2}}[HONO] \quad (14)$$

where A and B are constants written by

$$A = \frac{\gamma_d\omega}{2r} = \frac{3.657 D_g}{r^2}, B = \frac{\gamma_d\omega}{4H_{eff}RT}\sqrt{\frac{\bar{u}}{v}\frac{\pi}{D_{aq}}} \quad (15)$$

Then integrating eq 14 yields

$$\ln\frac{[HONO]}{[HONO]_0} = \frac{2A}{B^2}[\ln(1+Bt^{1/2}) - Bt^{1/2}] \quad (16)$$

In the present experiment, decrease in [HONO] due to the uptake was measured as a function of the gas−liquid contact distance, z. As the contact time for the gas is obtained by the relation $t = z/\bar{u}$, ln ([HONO]/[HONO]$_0$) experimentally obtained was plotted against t. Fitting eq 16 to the experimentally observed decay gave the values of A and B. It should be noted that t is shifted in each fitting process so as to obtain better fitting, because it is difficult to determine $t = 0$. We estimated the uptake coefficient, γ_w, from the value of B determined from the fitting for each pH. On the other hand, γ_w is obtained by using the known values of the parameters included in eq 8. Thus we compared γ_w values obtained in these two ways.

3. Results and Discussion

3.1. Relationship between Signal Intensities and HONO Concentration. As described in section 2.2, the HONO concentration in the gas phase was monitored by the chemical ionization mass spectrometer. To ensure the ability of the chemical ionization mass spectrometer to measure the HONO concentration, we investigated the relationship between the signal intensity and the concentration of HONO extracted from the flow tube without the liquid film prior to the uptake measurements. Figure 2 shows a mass spectrum of ions detected by the chemical ionization mass spectrometer, when the HONO concentration in the flow tube, [HONO], was 2.5×10^{12} molecules cm^{-3}. Ion peaks at $m/z = 99$ and 101 are assigned to the reagent ion, SO_2Cl^-, whereas those at $m/z = 82$ and 84 to $HONOCl^-$, the product ions by the reaction between SO_2Cl^- and HONO shown as eq 4. There are other ions than SO_2Cl^- and $HONOCl^-$ in Figure 2, which are not in the scope of our study. Ions at $m/z = 71$, 73, and 75 are assignable to $ClHCl^-$, which are produced by the chloride transfer reaction from SO_2Cl^- to HCl. It is highly likely that HCl is formed by the discharge of CH_3Cl at the ion source. In fact, $ClHCl^-$ appeared in the mass spectrum, even when HONO was not introduced in the flow tube. Trace amounts of water vapor reacts with the reagent ion to produce an adduct ion, $SO_2Cl^-(H_2O)$, which appears at $m/z = 117$ and 119.

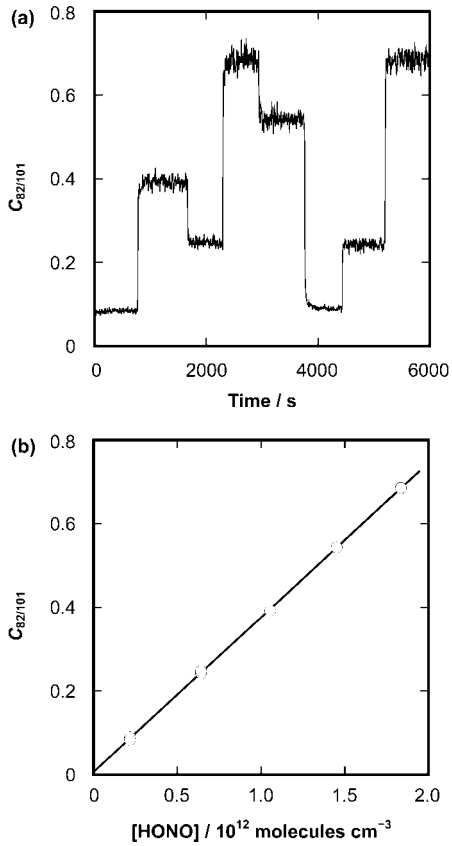

Figure 3. (a) Signal intensity of $HONOCl^-$ at $m/z = 82$ normalized by that of SO_2Cl^- at $m/z = 101$ ($C_{82/101}$) with time. Nitrous acid was prepared by the one pot synthesis using $NaNO_2$. The stepwise changes of $C_{82/101}$ were due to the changes of the concentration of HONO in the flow tube. (b) Plot of $C_{82/101}$ versus the concentration of HONO in the flow tube. There is a clear linear relationship between $C_{82/101}$ and the concentration of HONO in the concentration range studied.

The count rates of the ion signal were monitored by changing [HONO]. Because of the long-term drift of the intensity of SO_2Cl^-, the count rate of $HONOCl^-$ also changed with time, even when [HONO] was kept constant. However, the signal intensity of $HONOCl^-$ normalized by that of SO_2Cl^- was found to be proportional to [HONO]. Figure 3a shows the ratio of the count rate of the ions at $m/z = 82$ ($HONOCl^-$) to that at $m/z = 101$ (SO_2Cl^-) (hereafter referred as $C_{82/101}$) in response to the stepwise change of [HONO]. It was found that fluctuation of $C_{82/101}$ was below 3% as far as [HONO] was kept constant, indicating that both the preparation and detection of HONO were stable with time. Figure 3 (b) plots $C_{82/10}$ versus [HONO]. The plot shows clearly a linear relationship between $C_{82/101}$ and [HONO], which ensures that we can determine [HONO] from $C_{82/101}$.

3.2. Uptake of HONO by Aqueous Solution at pH = 7.1 and 11.1. Figure 4 shows the ratio $[HONO]/[HONO]_0$ after the flow tube as a function of the contact time for the gas, t, with the aqueous solution at the pH of 7.1 and 11.1. Evidently, the plots for the solution at pH = 7.1 and 11.1 exhibit a similar exponential decay with an increase in the contact time, t. It is confirmed by the semilogarithmic plot shown in the inset of Figure 4, in which the data points form a straight line. The slope of the plot was obtained from the least-squares fitting to be 2.06 $\pm$ 0.25 and 2.11 $\pm$ 0.24 s^{-1} for the solution at pH = 7.1 and 11.1, respectively. The slopes at pH = 7.1 and 11.1 are essentially same, implying that the same process determines the decay rate of HONO. If the decay rate was affected by the liquid

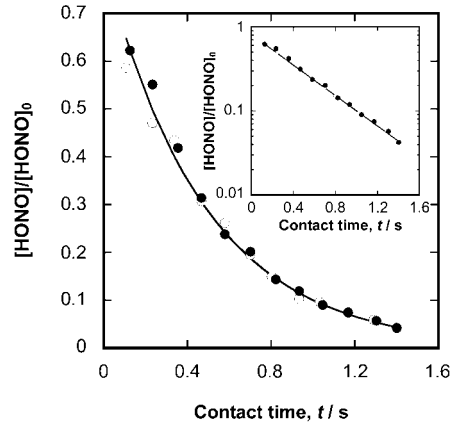

Figure 4. $[HONO]/[HONO]_0$ as a function of the contact time for the gas, t. The pH of the aqueous solution was prepared at 11.0 (solid circles) and 7.0 (open circles). Inset shows the semilogarithmic plot of the relative concentration of HONO, indicating that the $[HONO]/[HONO]_0$ decreases exponentially with the contact time.

phase processes, it should depend both on the contact time and on the pH of the solution. The present result indicates that the decay of HONO is limited only by the gas phase diffusion. Here, the slope of the plot is equal to the parameter A, which is related by eq 15 to the diffusion coefficient, D_g, of HONO in the carrier gas. The slopes at pH = 7.1 and 11.1 give D_g as 0.56 $\pm$ 0.07 $cm^2\ s^{-1}$ and 0.58 $\pm$ 0.07 $cm^2\ s^{-1}$, respectively. Because the gas mixture in the flow tube contains He, HONO, and water vapor, D_g is given as

$$\frac{1}{D_g} = \frac{P_{He}}{D_{HONO-He}} + \frac{P_{H_2O}}{D_{HONO-H_2O}} \qquad (17)$$

where $D_{HONO\text{-}He}$ and $D_{HONO\text{-}H_2O}$ are the pressure-independent diffusion coefficients of HONO in He and H_2O, respectively, and P_{He} and P_{H_2O} are the partial pressures of He and H_2O, respectively. Although these diffusion coefficients have not been measured as far as we know, Longfellow et al.[35] calculated $D_{HONO\text{-}He}$ and $D_{HONO\text{-}H_2O}$ at 220 K as 290 and 75 Torr $cm^2\ s^{-1}$, respectively. Assuming that the diffusion coefficients depend on $T^{1.75}$ as the expression for the binary diffusion coefficients obtained by Fuller et al.[36] based on the fitting to the experimental data, we can estimate $D_{HONO\text{-}He}$ and $D_{HONO\text{-}H_2O}$ at 294 K. Using these values and water vapor pressureP_{H_2O} = 18.7 Torr at 294 K, D_g was calculated to be 0.59 $cm^2\ s^{-1}$ at 294 K and 760 Torr. The experimentally obtained D_g agrees with the calculated one within uncertainties associated with the experiments and calculations. We thus average the values of D_g experimentally obtained at pH = 7.1 and 11.1 to obtain 0.57 $\pm$ 0.05 $cm^2\ s^{-1}$, which is then used for the following analysis. It should be noted that the diffusion coefficient determined here could be slightly overestimated because the liquid film with the small rippling can enhance the mass transport in the gas phase.

3.3. Uptake of HONO by Acidic Aqueous Solution at pH = 2.1−5.3. Figure 5 shows the semilogarithmic plot of the relative concentration $[HONO]/[HONO]_0$ as a function of the contact time for the gas, t, with aqueous solution at pH = 2.1−5.3. Obviously, the data points deviate from the single exponential decay observed for the aqueous solution at pH = 7.1 and 11.1. Also shown is that the decay rate depends on pH of the solution; the decay rate gets slower as the pH becomes lower. These results indicate that the uptake is affected by the liquid phase processes in addition to the gas phase diffusion. Thus we carried out a least-squares fitting of eq 16 to the

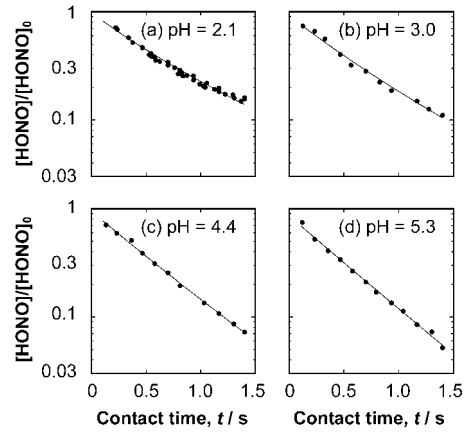

Figure 5. Semilogarithmic plot of $[HONO]/[HONO]_0$ as a function of the contact time for the gas, t, at different pH of the solution.

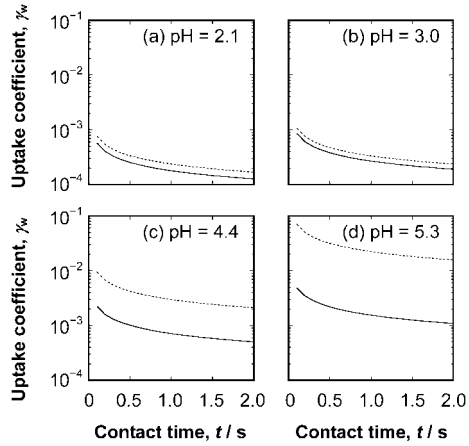

Figure 6. Uptake coefficient, γ_w, estimated from the fitting to the experimental data (solid lines) and from the calculation using known values of parameters involved (dotted lines) as a function of the contact time for the gas, t.

experimental data at each pH with B as the fitting parameter while the parameter A was fixed to the value calculated from D_g that was obtained in section 3.2. Best fitted curves are shown as solid lines in Figure 5 along with the experimental data.

Combining eqs 8 and 15 yields γ_w in terms of γ_d, B, and the contact time for the gas, t, as

$$\gamma_w = \frac{\gamma_d}{B}\sqrt{\frac{1}{t}} \tag{18}$$

Hence, we can estimate γ_w from the B values obtained above. The values of γ_w thus estimated are plotted as a function of the contact time for the gas, t, for each pH in Figure 6a−d with solid lines. On the other hand, γ_w can be calculated using eq 8 with the known values of the parameters. (Note that the conversion of the contact time is needed). In the calculation, Henry's law coefficient, H, and the acid dissociation constant, K_a, were estimated at 294 K from those at 298 K reported by Park and Lee[37] while aqueous phase diffusion coefficient of HONO, D_{aq}, was assumed to be equal to D_{aq} for NO_2^- (1.9×10^{-5} cm^2 s^{-1}) at 298 K.[38] The parameters for the calculation are summarized in Table 1. Dashed curves in Figure 6a−d show γ_w calculated using eq 8 for each pH. At pH = 2.1 and 3.0, γ_w values obtained by the experiment and the calculation agree fairly well considering uncertainties of the parameters used for the calculation. It is indicated that the uptake by the solution at pH = 2.1 and 3.0 is well described by the resistance model

TABLE 1: Parameters Used for the Calculation of γ_w

parameter	value
average gas flow velocity, $\bar{u}$	21.4 cm s^{-1}
liquid flow velocity at the interface, v	6.8 cm s^{-1}
temperature, T	294 K
average thermal speed of HONO, ω	3.6×10^4 cm s^{-1}
Henry's law coefficient, H	61 M atm^{-1}[a]
acid dissociation constant, K_a	4.9×10^{-4} M[a]
aqueous phase diffusion coefficient, D_{aq}	1.9×10^{-5} cm^2 s^{-1}[b]

[a] Estimated at 294 K from those at 298 K reported by Park and Lee.[37] [b] Reference 38.

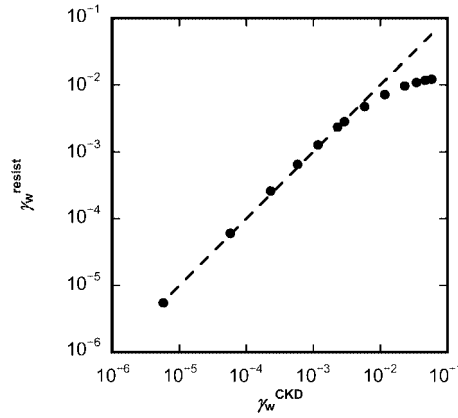

Figure 7. Logarithmic plot of γ_w^{resist} versus γ_w^{CKD}. Dashed line shows the 1:1 relation.

which includes the effects of the gas phase diffusion and wall loss processes. Also indicated is that the wall loss processes involves the physical absorption and the reversible acid dissociation reaction, both of which are considered to be in equilibrium.

At pH = 4.4 and 5.3, on the other hand, there is a discrepancy between the γ_w values obtained by two ways. The discrepancy seems to get larger as the pH of the solution becomes higher. In order to explain this discrepancy, possible causes are considered. First, we discuss the possibility that the γ_w value derived from the resistance model deviates from the true one. As described in section 2.4, one can estimate γ_w from the observed decay rate of the HONO concentration by the methods presented by Brown[24] or Murphy and Fahey,[23] both of which involve the effects of the gas phase diffusion using the continuity equation with appropriate boundary conditions. However, these models do not take the time dependent γ_w into consideration to correct for the effects of the gas phase diffusion. Hence, we adopted the resistance model in this work. Because γ_w is obtained by subtracting the effect of the gas phase diffusion from the overall uptake coefficient, γ_{tot}, it may have large uncertainty when the resistance of the gas phase diffusion is large. Therefore, we compare the time independent γ_w values derived from the resistance model, which is denoted as γ_w^{resist}, with those obtained from the CKD solution for the continuity equation presented by Murphy and Fahey,[23] which is denoted as γ_w^{CKD}. Figure 7 shows a plot of γ_w^{resist} versus γ_w^{CKD}, which ranges from 5×10^{-7} to 1×10^{-1}. For $\gamma_w^{CKD} \leq 3 \times 10^{-3}$, γ_w^{resist} is found to be equal to γ_w^{CKD}, demonstrating that the resistance model correctly describes the uptake rate controlled by both the gas phase diffusion and the wall loss process. For $\gamma_w^{CKD} > 3 \times 10^{-3}$, however, γ_w^{resist} is systematically lower than γ_w^{CKD}, suggesting that the analysis based on the resistance model underestimates the γ_w values. The resistance model underestimates the uptake rate at pH = 4.4 and 5.3 because γ_w values

larger than 3×10^{-3} are estimated from eq 8 using known values of the parameters involved. Nevertheless, the discrepancy is too large to be explained by the deviation of γ_w^{resist} from γ_w^{CKD}.

Second, we discuss possibility that the equilibrium in the liquid phase is not established. The expression of γ_w in eq 8 is derived under the assumption that the equilibrium of eq 3 is established at any points in the liquid in the course of the uptake. If the forward rate of eq 3 is so slow that the equilibrium is not established, the reaction should be regarded as an irreversible process to derive the uptake coefficient. Shi et al.[39] presented the uptake coefficient of weak acids or bases that includes the effects of the irreversible dissociation reactions based on the resistance model. According to their expression, the effects of the irreversible reactions become important when

$$\frac{1}{\sqrt{k_{aq}}} > > \frac{[H^+]}{K_a}\sqrt{\pi t'} \tag{21}$$

where k_{aq} is the first order rate coefficient for the forward reaction of eq 3. Note that eq 21 is written in terms of the contact time for the liquid, t'. As far as we know, the value of k_{aq} has not been reported for eq 3. On the other hand, the backward reaction of eq 3 can be assumed to be the aqueous-phase diffusion-limited reaction, for which the bimolecular rate coefficient is on the order of 10^{10} M^{-1} s^{-1}. From the backward rate coefficient and the equilibrium constant for eq 3, which corresponds to the acid dissociation constant, K_a, for HONO reported as on the order of 10^{-4} M,[37] k_{aq} is estimated to be $\sim 10^6$ s^{-1}. With this value, the term $1/\sqrt{k_{aq}}$ is $\sim 10^{-3}$, which is much smaller than the value of $[H^+]/K_a$ even at pH = 5. Noting that t' is around 1 s in the present experiments, one can conclude that the effects of k_{aq} are insignificant and cannot explain the observed discrepancy. In other words, K_a should be approximately 4 orders of magnitude larger than the reported value for the irreversible reaction rate to have effects on the uptake.

Finally, we discuss the possibility that physical and/or chemical properties near the surface are different from those in the bulk. It is known that the pH on the surface can be different from the pH in the bulk. Recent experimental[40−42] and theoretical[40,43−45] studies suggest that the pH of the air−water interface is lower than that in the bulk. Buck et al.[45] predicted pH < 4.8 at the surface of the neat water. We can estimate pH at the surface from the parameter B obtained by fitting eq 16 to the experimental data, assuming that other parameters than pH at the surface are the same as those for the bulk. For the aqueous solution with the bulk pH = 5.3 and 4.4, we estimate the pH at the surface as 4.1 and 3.7, respectively, which is consistent with the theoretical prediction. It is suggested that more acidic nature at the surface than the bulk may cause an additional resistance to the mass transfer of the weak acids such as HONO from the gas to the liquid phase. This is still qualitative speculation, so that further investigation is required.

4. Conclusions

Uptake kinetics of gas phase nitrous acid (HONO) by a pH-controlled aqueous solution was investigated by using a wetted wall flow tube coupled to the chemical ionization mass spectrometer. The uptake rate of the gaseous HONO was found to depend on the pH of the solution. For the uptake by neutral (pH = 7.1) and alkaline (pH = 11.1) solutions, the gas phase concentration was observed to decay exponentially, suggesting that the uptake was fully limited by the gas phase diffusion. On the other hand, the uptake by the acidic solution (pH = 2.1, 3.0, 4.4, and 5.3) was found to be affected by both the gas phase diffusion and the liquid phase processes including the physical absorption and acid dissociation reaction. The decay was analyzed by the rate equations based on the plug flow approximation and the resistance model with taking the time dependence of the uptake coefficient due to the saturation of the liquid surface into account. While the uptake processes by the solution at pH = 2.1 and 3.0 agree well with those calculated with the known values for the bulk liquid, the uptake rates by the solution at pH = 4.4 and 5.3 are found to be slower than the calculated ones. One possible explanation is that the lower pH at the liquid surface than that in the bulk liquid is responsible for the resistance of mass transfer from the gas to the liquid phase.

Acknowledgment. This work is partly supported by the Grant-in-Aid for Scientific Research (B) (no. 19350005 and 20310001) from Japan Society for the Promotion of Science (JSPS).

References and Notes

(1) Finlayson-Pitts, B. J. *Chem. Rev.* **2003**, *103*, 4801–4822.
(2) Jungwirth, P.; Tobias, D. J. *Chem. Rev.* **2006**, *106*, 1259–1281.
(3) Davidovits, P.; Kolb, C. E.; Williams, L. R.; Jayne, J. T.; Worsnop, D. R. *Chem. Rev.* **2006**, *106*, 1323–1354.
(4) Finlayson-Pitts, B. J.; Wingen, L. M.; Sumner, A. L.; Syomin, D.; Ramazan, K. A. *Phys. Chem. Chem. Phys.* **2003**, *5*, 223–242.
(5) Stemmler, K.; Ammann, M.; Donders, C.; Kleffmann, J.; George, C. *Nature* **2006**, *440*, 195–198.
(6) Stemmler, K.; Ndour, M.; Elshorbany, Y.; Kleffmann, J.; D'Anna, B.; George, C.; Bohn, B.; Ammann, M. *Atmos. Chem. Phys.* **2007**, *7*, 4237–4248.
(7) Cape, J. N.; Hargreaves, K. J.; Storeton-West, R.; Fowler, D.; Colvile, R. N.; Choularton, T. W.; Gallagher, M. W. *Atmos. Environ.* **1992**, *26A*, 2301–2307.
(8) Bongartz, A.; Kames, J.; Schurath, U.; George, Ch.; Mirabel, Ph.; Ponche, J. L. *J. Atmos. Chem.* **1994**, *18*, 149–169.
(9) Mertes, S.; Wahner, A. *J. Phys. Chem.* **1995**, *99*, 14000–14006.
(10) Sander, S. P.; Friedl, R. R.; Ravishankara, A. R.; Golden, D. M.; Kolb, C. E.; Kurylo, M. J.; Molina, M. J.; Moortgat, G. K.; Keller-Rudek, H.; Finlayson-Pitts, B. J.; Wine, P. H.; Huie, R. E.; Orkin, V. L. *Chemical Kinetics and Photochemical Data for Use in Atmospheric Studies, Evaluation Number 15*; Jet Propulsion Laboratory: Pasadena, CA, 2006.
(11) Garrett, B. C.; Schenter, G. K.; Morita, A. *Chem. Rev.* **2006**, *106*, 1355–1374.
(12) Utter, R. G.; Burkholder, J. B.; Howard, C. J.; Ravishankara, A. R. *J. Phys. Chem.* **1992**, *96*, 4973–4979.
(13) Müller, B.; Heal, M. R. *J. Phys. Chem. A* **2002**, *106*, 5120–5127.
(14) Danckwerts, P. V. *Gas-Liquid Reactions*; McGraw-Hill: New York, 1970.
(15) Breman, R. S.; de la Cantera, M. A. *Anal. Chem.* **1986**, *58*, 1533–1537.
(16) Taira, M.; Kanda, Y. *Anal. Chem.* **1990**, *62*, 630–633.
(17) Febo, A.; Perrino, C.; Gherardi, M.; Sparapani, R. *Environ. Sci. Technol.* **1995**, *29*, 2390–2395.
(18) Baker, J.; Ashbourn, S. F. M.; Cox, R. A. *Phys. Chem. Chem. Phys.* **1999**, *1*, 683–690.
(19) Kleffmann, J.; Becker, K. H.; Wiesen, P. *Atmos. Environ.* **1998**, *32*, 2721–2729.
(20) Howard, C. J. *J. Phys. Chem.* **1979**, *83*, 3–9.
(21) Hanson, D. R.; Ravishankara, A. R. *J. Phys. Chem.* **1993**, *97*, 12309–12319.
(22) Boniface, J.; Shi, Q.; Li, Y. Q.; Cheung, J. L.; Rattigan, O. V.; Davidovits, P.; Worsnop, D. R.; Jayne, J. T.; Kolb, C. E. *J. Phys. Chem. A* **2000**, *104*, 7502–7510.
(23) Murphy, D. M.; Fahey, D. W. *Anal. Chem.* **1987**, *59*, 2753–2759.
(24) Brown, R. L. *J. Res. Natl. Bur. Stand.* **1978**, *83*, 1–8.
(25) Davis, E. J. *J. Phys. Chem. A* **2008**, *112*, 1922–1932.
(26) Hanson, D. R.; Burkholder, J. B.; Howard, C. J.; Ravishankara, A. R. *J. Phys. Chem.* **1992**, *96*, 4979–4985.
(27) Scheer, V.; Frenzel, A.; Behnke, W.; Zetzsch, C.; Magi, L.; George, Ch.; Mirabel, Ph. *J. Phys. Chem. A* **1997**, *101*, 9359–9366.
(28) Gutzwiller, L.; George, Ch.; Rössler, E.; Ammann, M. *J. Phys. Chem. A* **2002**, *106*, 12045–12050.
(29) Fickert, S.; Helleis, F.; Adams, J. W.; Moortgat, G. K.; Crowley, J. N. *J. Phys. Chem. A* **1998**, *102*, 10689–10696.
(30) Leyssens, G.; Louis, F.; Sawerysyn, J.-P. *J. Phys. Chem. A* **2005**, *109*, 1864–1872.

(31) Pöschl, U.; Canagaratna, M.; Jayne, J. T.; Molina, L. T.; Worsnop, D. R.; Kolb, C. E.; Molina, M. J. *J. Phys. Chem. A* **1998**, *102*, 10082–10089.

(32) Thornberry, T.; Abbatt, J. P. D. *Phys. Chem. Chem. Phys.* **2004**, *6*, 84–93.

(33) Schwartz, S. E. *Chemistry of Multiphase Atmospheric Systems*; Jaeschke, W., Ed.; NATO ASI Series; Springer-Verlag: Berlin, 1986.

(34) Kolb, C. E.; Worsnop, D. R.; Zahniser, M. S.; Davidovits, P.; Keyser, L. F.; Leu, M.-T.; Molina, M. J.; Hanson, D. R.; Ravishankara, A. R.; Williams, L. R.; Tolbert, M. A. Laboratory Studies of Atmospheric Heterogeneous Chemistry. In *Progress and Problems in Atmospheric Chemistry*; Barker, J. R., Ed.; World Scientific: Singapore, 1995; Chapter 18, pp 771−875.

(35) Longfellow, C. A.; Imamura, T.; Ravishankara, A. R.; Hanson, D. R. *J. Phys. Chem. A* **1998**, *102*, 3323–3332.

(36) Fuller, E. N.; Schettler, P. D.; Giddings, J. C. *Ind. Eng. Chem.* **1966**, *58*, 18–27.

(37) Park, J.-Y.; Lee, Y.-N. *J. Phys. Chem.* **1988**, *92*, 6294–6302.

(38) *Handbook of Chemistry and Physics*, 81st ed.; Lide, D. R., Ed.; CRC Press: Boca Raton, FL, 2000.

(39) Shi, Q.; Davidovits, P.; Jayne, J. T.; Worsnop, D. R.; Kolb, C. E. *J. Phys. Chem. A* **1999**, *103*, 8812–8823.

(40) Mucha, M.; Frigato, T.; Levering, L. M.; Allen, H. C.; Tobias, D. J.; Dang, L. X.; Jungwirth, P. *J. Phys. Chem. B* **2005**, *109*, 7617–7623.

(41) Peterson, P. B.; Saykally, R. J. *J. Phys. Chem. B* **2005**, *109*, 7976–7980.

(42) Tarbuck, T. L.; Ota, S. T.; Richmond, G. L. *J. Am. Chem. Soc.* **2006**, *128*, 14519–14527.

(43) Dang, L. X. *J. Chem. Phys.* **2003**, *119*, 6351–6353.

(44) Petersen, M. K.; Iyengar, S. S.; Day, T. J. F.; Voth, G. A. *J. Phys. Chem. B* **2004**, *108*, 14804–14806.

(45) Buch, V.; Milet, A.; Vácha, R.; Jungwirth, P.; Devlin, J. P. *Proc. Natl. Acad. Sci.* **2007**, *104*, 7342–7347.

JP8051483